J|A|C|S
ARTICLES
Published on Web 01/19/2002

Rhodium Chemzymes: Michaelis−Menten Kinetics in Dirhodium(II) Carboxylate-Catalyzed Carbenoid Reactions

Michael C. Pirrung,* Hao Liu, and Andrew T. Morehead, Jr.†

Contribution from the Department of Chemistry, Levine Science Research Center, Duke University, Durham, North Carolina 27708-0317

Received June 28, 2001. Revised Manuscript Received September 17, 2001

Abstract: Rhodium carboxylate-mediated reactions of diazoketones involving cyclopropanation, C−H insertion, and aromatic C−C double bond addition/electrocyclic ring opening obey saturation (Michaelis−Menten) kinetics. Axial ligands for rhodium, including aromatic hydrocarbons and Lewis bases such as nitriles, ethers, and ketones, inhibit these reactions by a mixed kinetic inhibition mechanism, meaning that they can bind both to the free catalyst and to the catalyst−substrate complex. Substrate inhibition can also be exhibited by diazocompounds bearing these groupings in addition to the diazo group. The analysis of inhibition shows that the active catalyst uses only one of its two coordination sites at a time for catalysis. Some ketones exhibit the interesting property that they selectively bind to the catalyst−substrate complex. The similarity of the kinetic constants from different types of reactions with similar diazoketones, regardless of the linking unit or the environment of the reacting alkene, suggests that the rate-determining step is the generation of the rhodium carbenoid. A very useful rhodium carboxylate catalyst for asymmetric synthesis, $Rh_2(DOSP)_4$, shows slightly slower kinetic parameters than the achiral catalysts, implying that enantioselectivity of this catalyst is based on slowing reactions from one of the enantiotopic faces of the reactant, rather than any type of ligand-accelerated catalysis. A series of rhodium catalysts derived from acids with pK_as spanning 4 orders of magnitude give very similar kinetic constants.

The concept of a "chemzyme" was introduced by Corey[1] to describe oxazaborolidine catalysts that exhibit high enantioselectivity and serve as catalysts for their own enantioselective synthesis, and it received much attention.[2] A chemzyme has been subsequently defined as a specific molecule or complex that can catalyze a single chemical reaction for a particular chemical substrate with very high enantioselectivity and enantiospecificity at rates that approach "catalytic perfection".[3] The term has been applied to hetero-bimetallic complexes that enhance the reactivity of both reactants in the asymmetric Michael addition,[4] Lewis acid catalysts for hetero-Diels−Alder reactions,[5] and even to achiral aluminum phenoxide catalysts for conjugate allylation.[6] Chemzyme membrane reactors have been created from the oxazaborolidine chemzymes.[7] However, the kinetics of none of these catalytic systems have been examined to support their catalytic perfection. Reactions are generally regarded as catalytically perfected when they occur at the diffusion-controlled limit, which may be $\sim 10^8$ M^{-1} s^{-1} for macromolecular diffusion involving enzymes in water. Small molecule organic catalysts might offer a faster diffusion limit, $\sim 10^{10}$ M^{-1} s^{-1}. While enzymes often do exhibit exquisite enantioselectivity, their most characteristic behavior is Michaelis−Menten kinetics. Surprisingly, few purely chemical catalytic reactions have been examined for Michaelis−Menten or saturation behavior, despite the fact that many might be expected to exhibit saturation kinetics.

Conventional catalytic organic reaction processes that have been analyzed using saturation kinetics are listed in Table 1 along with their kinetic parameters. The range of selectivity constants, the apparent second-order rate constant for the reaction of the substrate with the catalyst to give the product, or k_{cat}/K_m, is 6 orders of magnitude, but they do not even approach the diffusion-controlled limit. The reactions studied include catalytic hydrogenation, redox reactions, phosphate hydrolysis, and the Sharpless asymmetric dihydroxylation. The effects of several potential inhibitors of this latter reaction were also studied; for example, 2-naphthyl *N*-methylamine has a $K_i = 1.6$ mM. Since virtually any catalytic reaction involving an associative/dissociative step could obey saturation kinetics, it is surprising that more systems have not been studied in this manner. We have studied the kinetics of catalytic chemical processes that have received wide attention in organic synthesis, the rhodium-mediated reactions of diazocompounds via carbenoid intermediates.[8]

† Current address: Department of Chemistry and Biochemistry, University of Maryland, College Park, MD 20742-2021.

(1) Corey, E. J.; Chen, C. P.; Reichard, G. A. *Tetrahedron Lett.* **1989**, *30*, 5547−50.
(2) Waldrop, M. M. *Science* **1989**, *245*, 354−5.
(3) Bugg, T. *An Introduction to Enzyme and Coenzyme Chemistry*; Blackwell Science: Oxford, U.K., 1997.
(4) Sasai, H.; Arai, T.; Satow, Y.; Houk, K. N.; Shibasaki, M. *J. Am. Chem. Soc.* **1995**, *117*, 6194−8.
(5) Yao, S.; Johannsen, M.; Audrain, H.; Hazell, R. G.; Jorgensen, K. A. *J. Am. Chem. Soc.* **1998**, *120*, 8599−605.
(6) Ooi, T.; Kondo, Y.; Maruoka, K. *Angew. Chem., Int. Ed. Engl.* **1997**, *36*, 1183−5.
(7) Woeltinger, J.; Bommarius, A. S.; Drauz, K.; Wandrey, C. *Org. Process Res. Dev.* **2001**, *5*, 241−8.
(8) Pirrung, M. C.; Morehead, A. T. *J. Am. Chem. Soc.* **1996**, *118*, 8162−3.

10.1021/ja011599l CCC: $22.00 **© 2002 American Chemical Society**

Table 1. Kinetic Parameters for Selected Catalytic Reactions Exhibiting Saturation Kinetics

reaction	K_m (mM)	k_{cat} (s^{-1})	k_{cat}/K_m ($M^{-1}s^{-1}$)	ref
acrylamide/$HRuCl(diop)_2$	0.32	8.60×10^{-3}	2.7×10	9
acrylamide/$[HRuCl(PPh_3)_2]_2$	0.67	1.10×10^{-3}	1.6	9
flavin mimic/NADH analogue	101	3.65×10^{-5}	3.61×10^{-4}	10
thiol/cobalt−phthalocyanine	44.4	3.13×10^{-3}	7.05×10^{-2}	11
thiol/iron−phthalocyanine	9.64	6.75×10^{-4}	7.00×10^{2}	11
styrene/asymmetric dihydroxylation	17	2.60×10^{-1}	1.5×10	12
copper polymer/phosphate hydrolysis	8.77	4×10^{-2}	5	13
Cu-catalyzed Diels−Alder[a]	0.86	2.56×10^{-3}	2.97	14
Mo-catalyzed olefin epoxidation	48	53.3	1.1×10^{3}	15

[a] The k_{obs} for this bimolecular reaction was scaled by 1 mM cyclopentadiene.

Scheme 1

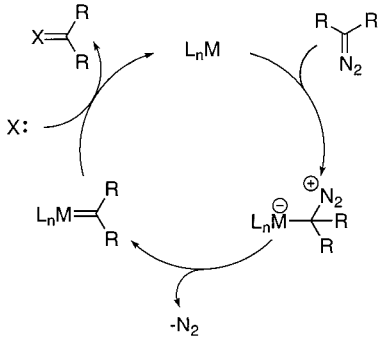

Several reviews of transition metal catalysis in carbenoid chemistry, particularly rhodium catalysis, are available.[16−18] The currently accepted mechanism of these reactions was first proposed by Yates (Scheme 1)[19] and invokes nucleophilic attack by the diazo compound on the electrophilic metal. After loss of nitrogen, the carbenoid reacts with an electron-rich substrate X and regenerates the catalyst. The dirhodium(II) carboxylates possess a "lantern" structure, with the two rhodium atoms surrounded by four carboxylates in a nominal D_4 symmetry and bearing two open axial coordination sites. Two extensive reviews of rhodium(II) complexes are available.[20]

The current understanding of the mechanisms of reactions of diazo compounds catalyzed by dirhodium(II) carboxylates is certainly incomplete, with the primary studies based on relative reactivity comparisons between potential substrates and inferences about the reactive species. Studies of regioselectivity,[21] enantioselectivity,[22] and chemoselectivity[23] in rhodium-mediated reactions have shown that an impressive degree of control can be exerted by the ligands. True mechanistic understanding of these reactions is complicated by the highly reactive nature of the intermediates, their low concentrations, and the multitude of potential reaction pathways. In some cases, these reaction pathways have been analyzed using theoretical methods.[24] Initial mechanistic study of the catalytic reactions of diazo compounds by rhodium carboxylates was performed by Hubert and Noels.[25] The kinetic parameters of the cyclopropanation of styrene with ethyl diazoacetate (EDA) catalyzed by rhodium acetate were determined to be $\Delta H^{\ddagger} = 15.0 \pm 0.6$ kcal/mol and $\Delta S^{\ddagger} = -3.1 \pm 2$ eu (0 °C). They also determined that this reaction is first order in catalyst. Subsequently, Alonso and García examined the rhodium acetate-catalyzed C−H insertion reaction of ethyl diazoacetate into dioxane and determined that the reaction is first order in EDA.[26] The kinetic parameters were determined to be $\Delta H^{\ddagger} = 16.4 \pm 1.4$ kcal/mol and $\Delta S^{\ddagger} = -25 \pm 4$ eu. The large negative entropy of activation for this reaction was attributed to a rate-determining step that does not involve nitrogen loss. These workers postulated a mechanism in which the rhodium acetate dimer is split to give a catalytically active monomeric catalyst. However, splitting of the dimer is not now widely believed to be involved in the mechanism.

Yates' model for diazo compound transformation can be applied to the catalytic cycle for rhodium(II) catalysts. If the first step is a reversible equilibrium complexation of the negatively polarized carbon of the diazocompound with the rhodium(II) catalyst and the second is a rate-determining loss of dinitrogen (Scheme 1), these processes should obey saturation kinetics. This study first aimed to evaluate this possibility; if Michaelis−Menten behavior could be shown, determination of the influence of catalyst and reactant structure on kinetic properties would be undertaken. These could contribute to understanding of the process of diazo loss, elucidate the role of the metal in facilitating the process, and identify the presence of any intermediates. Other concepts from Michaelis−Menten

(9) (a) Hui, B. C.; James, B. R. *Can. J. Chem.* **1974**, *52*, 3760−8. (b) James, B. R.; Wang, D. K. W. *Can. J. Chem.* **1980**, *58*, 245−50. (c) James, B. R.; Wang, D. K. W. *J. Chem. Soc., Chem. Commun.* **1977**, 550−1. (d) Joshi, A. M.; MacFarlane, K. S. James, B. R. *J. Organomet. Chem.* **1995**, *488*, 161−7.
(10) Shinkai, S.; Ishikawa, Y.; Shinkai, H.; Tsuno, T.; Makishima, H.; Ueda, K.; Manabe, O. *J. Am. Chem. Soc.* **1984**, *106*, 1801−8.
(11) Hanabusa, K.; Ye, X.; Koyama, T.; Kurose, A.; Shirai, H.; Hojo, N. *J. Mol. Catal.* **1990**, *60*, 127−34.
(12) Corey, E. J.; Noe, M. C. *J. Am. Chem. Soc.* **1996**, *118*, 319−29.
(13) Menger, F. M.; Tsuno, T. *J. Am. Chem. Soc.* **1989**, *111*, 4903−7.
(14) Otto, S.; Bertoncin, F.; Engberts, J. B. F. N. *J. Am. Chem. Soc.* **1996**, *118*, 7702−7.
(15) (a) Su, C.-C.; Reed, J. W.; Gould, E. S. *Inorg. Chem.* **1973**, *12*, 337−42. (b) Arakawa, H.; Moro-oka, Y.; Ozaki, A. *Bull. Chem. Soc. Jpn.* **1974**, *47*, 2958−2961.
(16) Doyle, M. P. *Chem. Rev.* **1986**, *86*, 919−39.
(17) (a) Adams, J.; Spero, D. M. *Tetrahedron* **1991**, *47*, 1765−808. (b) Padwa, A.; Krumpe, K. E. *Tetrahedron* **1992**, *48*, 5385−453.
(18) (a) Doyle, M. P. *Acc. Chem. Res.* **1986**, *19*, 348. (b) Padwa, A.; Hornbuckle, S. F. *Chem. Rev.* **1991**, *91*, 263−309. (c) Maas, G. *Top. Curr. Chem.* **1987**, *137*, 75.
(19) Yates, P. *J. Am. Chem. Soc.* **1952**, *74*, 5376−81.
(20) (a) Felthouse, T. R. *Prog. Inorg. Chem.* **1982**, *29*, 74−166. (b) Jardine, F. H.; Sheridan, P. S. In *Comput. Coord. Chem.*; Wilkinson, G., Ed.; Pergamon Press: New York, 1987; Vol. IV, pp 934−1083.
(21) (a) Doyle, M. P.; Westrum, L. J.; Wolthuis, W. N. E.; See, M. M.; Boone, W. P.; Bagheri, V.; Pearson, M. M. *J. Am. Chem. Soc.* **1993**, *115*, 958−64. (b) Taber, D. F.; Hennessy, M. J.; Louey, J. P. *J. Org. Chem.* **1992**, *57*, 436−41. (c) Taber, D. F.; Hoerner, R. S. *J. Org. Chem.* **1992**, *57*, 441. (d) Hashimoto, S.; Watanabe, N.; Ikegami, S. *Tetrahedran Lett.* **1992**, *33*, 2709−12. (e) Ceccherelli, P.; Curini, M.; Marcotullio, M. C.; Rosati, O. *Tetrahedran* **1991** *47*, 7403−8. (f) Doyle, M. P.; Pieters, R. J.; Taunton, J.; Pho, H. Q.; Padwa, A.; Hertzog, D. L.; Precedo, L. *J. Org. Chem.* **1991**, *56*, 820. (g) Demonceau, A.; Noels, A. F.; Hubert, A. J. *Tetrahedron* **1990**, *46*, 3889−96. (h) Doyle, M. P.; Bagheri, V.; Wandless, T. J.; Harn, N. K.; Brinker, D. A.; Eagle, C. T.; Loh, K. *J. Am. Chem. Soc.* **1990**, *112*, 1906−12. (i) Doyle, M. P.; Bagheri, V.; Pearson, M. M.; Edwards, J. D. *Tetrahedron Lett.* **1989**, *30*, 7001−4. (j) Demonceau, A.; Noels, A. F.; Hubert, A. J.; Teyssié, P. *Bull. Chem. Soc. Belg.* **1984**, *93*, 945−8.
(22) For reviews see: Doyle, M. P. *Recl. Trav. Chim. Pays-Bas* **1991**, *110*, 305−16. Brunner, H. *Angew. Chem., Int. Ed. Engl.* **1992,** *31*, 1183−5.
(23) (a) Padwa, A.; Austin, D. J.; Price, A. T.; Semones, M. A.; Doyle, M. P.; Protopopova, M. N.; Winchester, W. R.; Tran, A. *J. Am. Chem. Soc.* **1993**, *115*, 8669−80. (b) Padwa, A.; Austin, D. J.; Hornbuckle, S. F.; Semones, M. A.; Doyle, M. P.; Protopopova, M. N. *J. Am. Chem. Soc.* **1992**, *114*, 1874−6. (c) Reference 21b. (d) Hashimoto, S.; Watanabe, N.; Ikegami, S. *J. Chem. Soc., Chem. Commun.* **1992**, 1508−10. (e) Doyle, M. P.; Taunton, J.; Pho, H. Q. *Tetrahedron Lett.* **1989**, *30*, 5397−400. (f) Cox, G. G.; Moody, C. J.; Austin, D. J.; Padwa, A. *Tetrahedron* **1993**, *49*, 5109−26. (g) Doyle, M. P.; Pieters, R. J.; Taunton, J.; Pho, H. Q.; Padwa, A.; Hertzog, D. L.; Precedo, L. *J. Org. Chem.* **1991**, *56*, 820−9. (h) Doyle, M. P.; Bagheri, V.; Wandless, T. J.; Harn, N. K.; Brinker, D. A.; Eagle, C. T.; Loh, K. L. *J. Am. Chem. Soc.* **1990**, *112*, 1906−12.
(24) Padwa, A.; Snyder, J. P.; Curtis, E. A.; Sheehan, S. M.; Worsencroft, K. J.; Kappe, C. O. *J. Am. Chem. Soc.* **2000**, *122*, 8155−67.
(25) Anciaux, A. J.; Hubert, A. J.; Noels, A. F.; Petiniot, N.; Teyssié, P. *J. Org. Chem.* **1980**, *45*, 695−702.
(26) Alonso, M. E.; García, M. del C. *Tetrahedron* **1989**, *45*, 69−76.

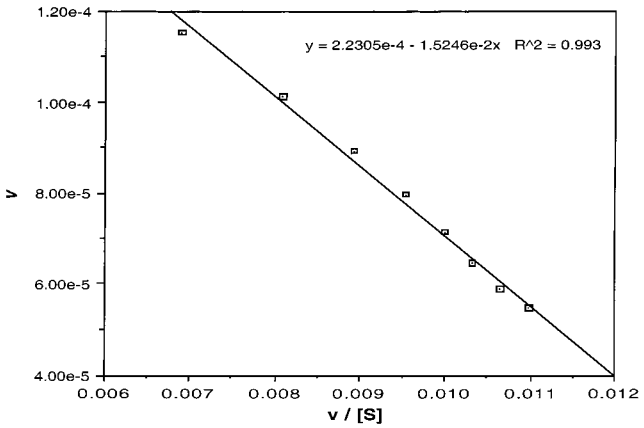

Figure 1. Eadie−Hofstee plot of the rate of reaction of diazoketone **1** catalyzed by rhodium pivalate at low substrate concentration [5−25 mM].

Scheme 2

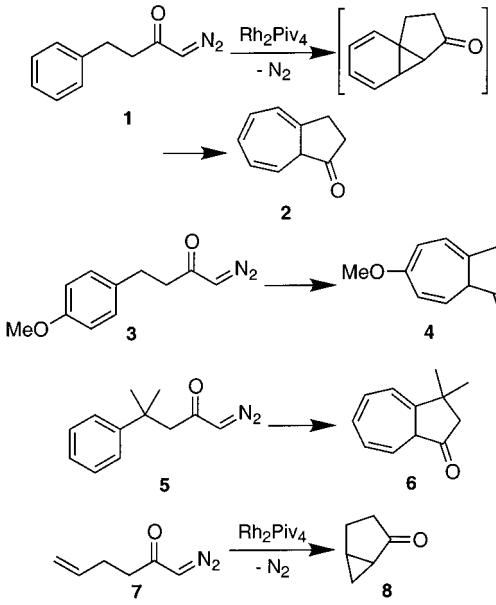

kinetics, including the study of Lewis basic inhibitors, could also be applied, and the factors affecting the kinetic "perfection" of these catalysts could be evaluated.

Results

The intramolecular Büchner reaction of diazoketone **1** to produce **2** (Scheme 2), introduced by McKervey,[27] was well suited to begin this study. It proceeds in high yields (>95%) at room temperature, and product appearance is easily followed at 340 nm, at which the wavelength of product **2** has a much greater absorbance ($\epsilon = 187\ M^{-1}\ cm^{-1}$) than the reactant ($\epsilon = 37\ M^{-1}\ cm^{-1}$). Reactions were performed at substrate concentrations from 5 to 25 mM in methylene chloride, catalyzed by rhodium pivalate (0.2 μM). This rhodium carboxylate and all those studied here fully dissolve in noncoordinating and nonpolar solvents, in this case dichloromethane, so that catalyst concentrations can be precisely calculated. Product formation was followed by UV to <10% conversion, ensuring the rates measured are initial rates. A direct kinetic plot of this reaction (v vs [S]) shows a hyperbolic form, supporting the hypothesis that rhodium-catalyzed diazoketone reactions exhibit saturation kinetics. An Eadie−Hofstee plot (Figure 1) was used to determine the kinetic parameters (Table 2).[28] The saturation kinetic model was further supported by study of the intramolecular Büchner reaction of compounds **3** and **5**, which produce the hydroazulene derivatives **4** and **6** in high yield. Both show kinetic parameters essentially identical to **1**.

Table 2. Saturation Kinetic Parameters for Intramolecular Büchner and Cyclopropanation Reactions[a]

reactant/catalyst	K_m (mM)	k_{cat} (s^{-1})	k_{cat}/K_m ($M^{-1}\ s^{-1}$)	$K_{i(S)}$ (mM)
1/Rh_2Piv_4	15	1100	7.3×10^4	265
3/Rh_2Piv_4	15	1090	7.3×10^4	96
5/Rh_2Piv_4	13	1170	9.0×10^4	
7/Rh_2Piv_4	14	1120	8.0×10^4	
1/Rh_2TCA_4	1	625	6.25×10^5	10

[a] CH_2Cl_2 solvent, room temperature.

The rhodium-catalyzed reactions of **3** and **5** would be expected to show different rate constants than that of **1** if carbon−carbon bond formation were rate limiting. The electron-donating methoxy group would be expected to increase the rate of electrophilic attack on the aryl ring in **3**, and the *gem*-dimethyl effect[29] would be expected to increase the rate of attack on the phenyl ring in **5**. With the exception of the substrate inhibition parameters (vide infra), both **3** and **5** have kinetic parameters virtually identical to **1**, indicating that the rate-determining step occurs before the attack on the aromatic ring. One caution should be added concerning this intermediate conclusion, however. The Büchner reaction involves an initial formation of the norcaradiene by cyclopropanation,[30] followed by electrocyclic ring opening to the cycloheptatriene. If the cyclopropanation step were fast and the ring opening rate determining, similar saturation kinetic behavior could be observed. It therefore seemed prudent to examine a second reaction that could obey saturation kinetics and was not subject to an alternative reaction pathway.

The rhodium-catalyzed reaction of **7** to give **8** was examined under conditions (0.2 μM rhodium pivalate, methylene chloride) identical to those of the earlier reactions. In this case, the loss of the diazo compound was followed spectrophotometrically at 370 nm. The kinetic parameters for this reaction are in excellent agreement (<3% standard deviation in k_{cat}) with those for the Büchner reactions.

The dirhodium(II)-catalyzed intramolecular Büchner reaction and cyclopropanation obey saturation kinetics. The kinetic constants are insensitive to aromatic substitution in the Büchner reaction and are nearly identical for both the Büchner reaction and cyclopropanation. The simplest model that fits these results is equilibrium complexation of the diazo compound with the metal followed by dissociation of molecular nitrogen to generate the rhodium carbenoid, as previously postulated by Yates; the latter step must be the rate-determining step. However, it is conceivable that other dissociative processes are rate limiting in these rhodium-catalyzed reactions. For example, it is known

(27) (a) McKervey, M. A.; Tuladhar, S. M.; Twohig, M. F. *J. Chem. Soc., Chem. Commun.* **1984**, 129−30. (b) Kennedy, M.; McKervey, M. A. Maguire, A. R.; Tuladhar, S. M.; Twohig, M. F. *J. Chem. Soc., Perkin Trans. 1* **1990**, 1047−54.

(28) Abbreviations used in tables: Piv: pivalate; TCA: trichloroacetate; Oct: octanoate; OBz: benzoate; OBz-F: *p*-fluorobenzoate; TFA: trifluoroacetate; Ac: acetate; DOSP: tetrakis(*S*−(*N*-dodecylbenzenesulfonyl)prolinate).

(29) Jung, M. E.; Gervay, J. *J. Am. Chem. Soc.* **1991**, *113*, 224−32.

(30) For the first isolation of a norcaradiene intermediate in this reaction and further citations to it, see: Manitto, P.; Monti, D.; Speranza, G. *J. Org. Chem.* **1995**, *60*, 484−5.

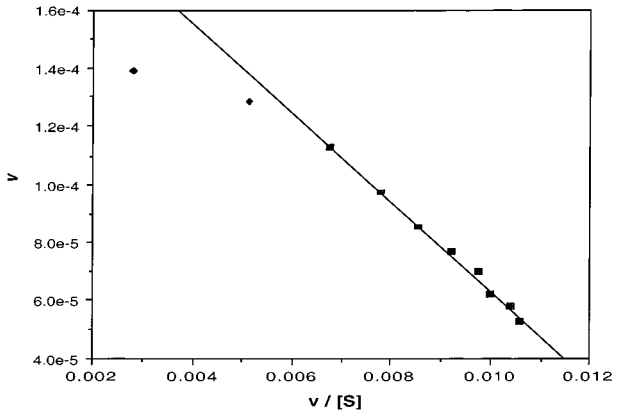

Figure 2. Eadie−Hofstee plot of the reaction of diazoketone **3** catalyzed by rhodium pivalate at low substrate concentration [5−25 mM].

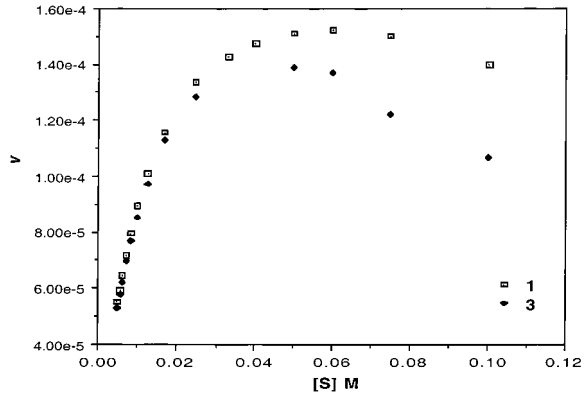

Figure 3. Direct plots of the velocity of the reaction of diazoketones **1** and **3** catalyzed by rhodium pivalate at high substrate concentration [5−100 mM].

that the rate of formation of phosphine and nitrogenous base adducts of dirhodium carboxylates in water and acetonitrile is controlled by dissociation of the solvent from the axial coordination sites.[31] In an alternative kinetic scheme (Scheme 3), the initial dissociation of the solvent would be followed by kinetically significant product formation. However, methylene chloride is a very poorly coordinating solvent, and it is unlikely that $K_m = 15$ mM could be attributed to the desolvation of the catalyst. The rhodium pivalate had been freed of the axial waters before use by heating under vacuum, so the dissociation of water is not the source of the saturation kinetics observed. The lack of a dependence of the kinetic constants on the particular aromatic group in the diazoketone suggests that kinetic constants characteristic of each diazo compound−catalyst combination but independent of the type of chemical reaction (C−H insertion or cyclopropanation) will be obtained because the rate-determining step is the formation of the carbenoid.

In initial studies of **3**, a lower than expected rate was observed at the higher concentrations of substrate. An Eadie−Hofstee plot (Figure 2) shows this nonlinear dependence at the two highest concentrations. Data were therefore collected at even higher substrate concentrations, producing the direct plots for **1** and **3** shown in Figure 3. The effect is particularly pronounced with **3**. One possible mechanism that could result in such an effect is nonproductive binding of the substrate to the catalyst

Scheme 3

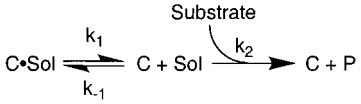

Scheme 4

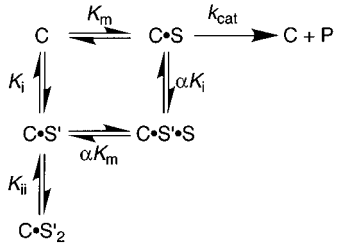

(substrate inhibition). The potential nonproductive binding sites on these substrate molecules include the carbonyl, the terminal nitrogen of the diazo group, and the aromatic ring. That the substrate inhibition of rhodium pivalate catalysis appears at lower substrate concentrations for the 4-methoxy substituted compound **3** than for the simple phenyl substituted compound **1** suggests the nonproductive binding site is the aromatic ring. Kinetic determination of the K_is for the substrate inhibition of rhodium pivalate catalysis was accomplished by extrapolating the linear portions of $1/v$ vs [S] plots to their x-axis intercept.[32] Compound **3** (96 mM) has a lower substrate K_i than **1** (265 mM), supporting the postulated mechanism of inhibition by binding of the aromatic ring to the catalyst. If inhibition were occurring through binding of the carbonyl or diazo group to the catalyst, **1** and **3** should exhibit substrate inhibition to the same extent. Compound **5** demonstrates no substrate inhibition with rhodium pivalate catalysis, which may be due to increased steric demand of the quaternary carbon-substituted aromatic ring, preventing binding to the catalyst.

A general inhibition scheme that fits these data is shown in Scheme 4, in which the substrate bound in a nonproductive manner is indicated by S′. Nonproductive binding of a single substrate molecule to the catalyst would result in simple mixed inhibition kinetics (vide infra). Binding of a second substrate nonproductively would prevent formation of the possibly productive C·S·S′ complex, which could also lose S′ to give the catalytically competent C·S. The inhibition observed for rhodium pivalate catalysis at the high concentrations of substrate results in linear $1/v$ vs [S] plots, indicating the second nonproductive binding event does not occur to a significant extent.

To further probe this substrate inhibition process, rhodium trichloroacetate was examined as a catalyst in the reaction of **1**. Owing to its greater Lewis acidity than rhodium pivalate, it would be predicted to bind the aromatic ring more strongly. The parabolic v vs [S] direct plot shows strong substrate inhibition (Figure S1, Supporting Material). Use of the linear portion of the Eadie−Hofstee plot (at low [S], Figure S2) allowed the kinetic constants to be determined. This more electron-deficient catalyst gives a lower K_m and k_{cat} (Table 2), but the selectivity constant is about 10-fold greater than that of rhodium pivalate. The method of Dixon and Webb[32] was used to calculate $K_{i(S)}$ for rhodium trichloroacetate catalysis, which is 30-fold lower than with the pivalate (determined at substrate

(31) (a) Das, K.; Simmons, E. L.; Bear, J. L. *Inorg. Chem.* **1977**, *16*, 1268−71. (b) Aquino, M. A. S.; Macartney, D. H. *Inorg. Chem.* **1987**, *26*, 2696−9. (c) Aquino, M. A. S.; Macartney, D. H. *Inorg. Chem.* **1988**, *27*, 2868−72.

(32) Dixon, M.; Webb, E. C. *Enzymes*; Academic Press: New York, 1979; pp 126−36.

Scheme 5

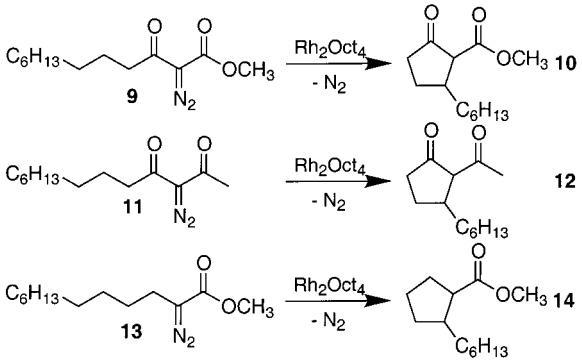

Table 3. Dependence of Saturation Kinetic Parameters on Diazocarbonyl Structure

reactant/catalyst	K_m (mM)	k_{cat} (s^{-1})	k_{cat}/K_m ($M^{-1}s^{-1}$)
1/Rh_2Oct_4	9.5	151	1.6×10^4
9/Rh_2Oct_4	124	15	1.2×10^2
11/Rh_2Oct_4	71	5.9	8.3×10

concentrations > 50 mM). Since the plot of $1/v$ vs [S] used to determine $K_{i(S)}$ is linear at higher concentrations (Figure S3), $K_{ii(S)}$ must be higher than 25 mM and is not a significant contributor to inhibition in this case. It is well-established that binding of one Lewis basic axial ligand to rhodium disfavors the second axial binding by 10−100 times, and presumably the second binding could occur only at high substrate concentrations.[33]

Further evidence regarding substrate inhibition was gained by a second, intermolecular inhibition study. If substrate inhibition arises via nonproductive binding of the aromatic ring to the catalyst, then another aromatic compound should also be able to act as an inhibitor. The reaction of **5** catalyzed by rhodium pivalate was examined in the presence of anisole. The method of Dixon[32] was used to determine the anisole K_i, which is 107 mM, in reasonable agreement with the K_i for substrate inhibition by **3** of 96 mM. Further studies of inhibition by Lewis bases are given later.

Other types of diazo compounds were examined to determine the influence of structure on saturation kinetic properties. Diazo-β-ketoester **9** was prepared by dianion alkylation of ethyl acetoacetate and diazo transfer, as was the diazo-β-diketone **11**. Their intramolecular C−H insertion reactions (Scheme 5) were examined by following the loss of the diazocarbonyl absorption in the UV with Rh_2Oct_4 as catalyst and compared with the Büchner reaction of **1**. Results are summarized in Table 3. Weak substrate inhibition (too weak to be accurately determined) was observed with **9** and **11**, but not with **1**, as contrasted with its reaction catalyzed by rhodium pivalate. The C−H insertion reaction of **13** was also examined but proved too rapid to be studied with the methods used here.

One of the most powerful new synthetic technologies based upon rhodium-catalyzed reactions of diazo compounds exploits chiral catalysis. The rhodium prolinate family of catalysts developed by Davies show good enantioselectivity in reactions of vinyl or aryl diazocarbonyls such as cyclopropanation and C−H insertion.[34] Methyl phenyldiazoacetate (**15**, Scheme 6)

Scheme 6

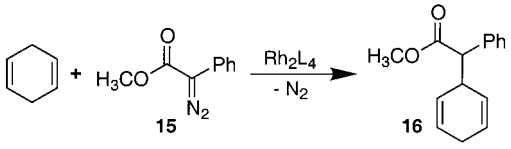

Table 4. Saturation Kinetic Parameters for Reactions of Methyl Phenyldiazoacetate with an Asymmetric Catalyst and Achiral Catalysts

reactant/catalyst	K_m (mM)	k_{cat} (s^{-1})	k_{cat}/K_m ($M^{-1}s^{-1}$)
15/$Rh_2(DOSP)_4$	24.7	1.58	6.40×10
15/Rh_2Piv_4	9.07	1.29	1.42×10^2
15/Rh_2Oct_4	9.08	1.27	1.39×10^2

Table 5. Dependence of Saturation Kinetic Parameters on Dirhodium Carboxylate Catalysts in Reactions of **1**

catalyst	K_m (mM)	k_{cat} (s^{-1})	k_{cat}/K_m ($M^{-1}s^{-1}$)	RCO_2H pK_a
Rh_2Piv_4	7.53	101	1.33×10^4	5.03
Rh_2Oct_4	9.53	151	1.58×10^4	4.89
$Rh_2(OBz)_4$	6.34	92.2	1.45×10^4	4.19
$Rh_2(OBz-p\text{-}F)_4$	6.08	121	2.00×10^4	2.90
Rh_2TFA_4	3.51	70.9	2.02×10^4	0.67

insertion into C−H bonds is catalyzed by rhodium prolinates with good to excellent enantioselectivity.[35] Müller carried out the reaction of 1,4-cyclohexadiene (20 equiv) with **15** promoted by the chiral rhodium prolinate catalyst $Rh_2(DOSP)_4$ (in 65% ee and 98% yield) by adding the diazo compound to a solution of cyclohexadiene and catalyst via a syringe pump. Since it is known that vinyl and aryl diazocarbonyls are not prone to carbene dimerization,[36] saturation kinetics studies of this reaction could be performed by addition of the catalyst to a mixture of the two reactants. Under these conditions with rhodium pivalate, the C−H insertion product **16** is obtained in 88% isolated yield. The kinetics of the reaction promoted by a chiral and two achiral catalysts were examined using methods similar to those applied to **1**. The kinetic parameters are summarized in Table 4.

The foregoing was our first study of the effect of significant catalyst variations on the kinetics of a dirhodium carboxylate-catalyzed reaction. It seemed worthwhile to examine a wider range of catalyst variants in the reaction of **1** for comparison. These experiments were performed under slightly different conditions but similar to those previously used. The results are summarized in Table 5. Substrate inhibition occurs at concentrations > 50 mM, and $K_{i(S)}$ was determined in the case of Rh_2TFA_4 to be 48 mM.

The discovery that rhodium-catalyzed reactions of diazo compounds could be inhibited by Lewis bases as weak as anisole suggested examination of the inhibition by other weak Lewis bases, with the further attraction of potentially providing insight into the mechanism of rhodium carboxylate catalysis. Because dirhodium complexes have two open axial coordination sites, they could conceivably catalyze diazo compound reactions at both sites. Strong ligands such as imidazoles, sulfides, and phosphines completely abolish catalytic activity, presumably through coordination at both axial sites. It has also been shown that binding of a Lewis basic ligand (which might be extended

(33) Drago, R. S.; Long, L. R.; Cosmano, R. *Inorg. Chem.* **1981**, *20*, 2920−7
(34) Davies, H. M. L.; Antoulinakis, E. G. *J. Organomet. Chem.* **2001**, *617*−*8*, 47−55. Davies, H. M. L. *Eur. J. Org. Chem.* **1999**, 2459−69.
(35) Davies, H. M. L.; Hansen, T.; Churchill, M. R. *J. Am. Chem. Soc.* **2000**, *122*, 3063−70. Müller, P.; Tohill, S. *Tetrahedron* **2000**, *56*, 1725−31.
(36) Davies, H. M. L.; Hodges, L. M.; Matasi, J. J.; Hansen, T.; Stafford, D. G. *Tetrahedron Lett.* **1998**, *39*, 4417.

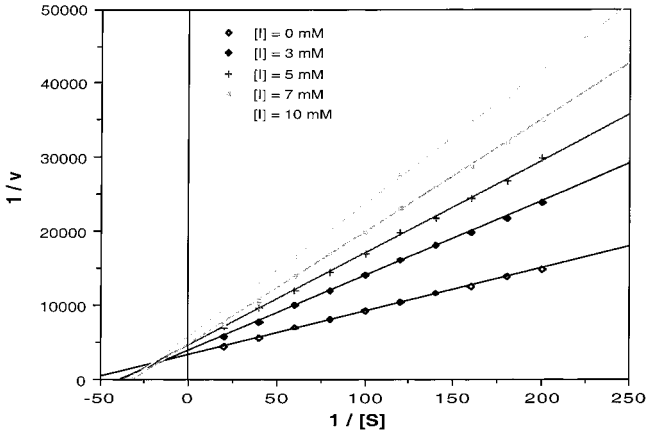

Figure 4. Lineweaver−Burk plot of the inhibition by acetonitrile of the reaction catalyzed by rhodium pivalate of diazoketone **5**.

Scheme 7

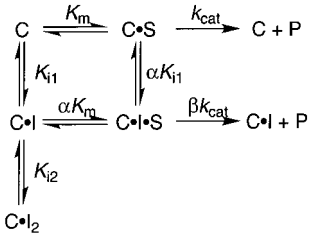

to include the carbenoid) at one site weakens binding at the other site (via the trans effect), suggesting that only one site might be catalytically active at any given time. Since this influence would be analogous to competitive inhibition (weakening binding = raising K_m), the study of the effect of a Lewis base on the kinetics could lend insight into the mechanism.

With two possible inhibitor binding sites, the kinetics of these reactions can be complex. A general analysis for this system is given in Scheme 7, and its detailed analysis is presented in the Supporting Information. Besides the conventional Michaelis−Menten constants, two key parameters of the kinetics of this system are α and β. The former classifies inhibition based on the position of the intersection of double reciprocal lines at multiple inhibitor concentrations. For mixed inhibition, the point of intersection is in the second quadrant if $\alpha > 1$, and it is in the third quadrant if $\alpha < 1$. If the point of intersection is on the $-x$ axis, $\alpha = 1$, and this is noncompetitive inhibition. If $\alpha = \infty$, the point of intersection is on the $+y$ axis and the situation simplifies greatly to competitive inhibition. The value of β exemplifies the catalytic power of a ternary complex with substrate and inhibitor.

The weak ligand acetonitrile was examined in the rhodium pivalate-catalyzed reaction of **5** (chosen because it is not complicated by substrate inhibition). The reaction was performed in the presence of 3.00, 5.00, 7.00, and 10.0 mM of acetonitrile in dichloromethane, under conditions otherwise identical to those employed previously. The resultant v vs [S] plots are shown in Figure S4 (Supporting Information), and double reciprocal plots of these data are shown in Figure 4. Graphic analysis indicates mixed inhibition. Replots of the slope and intercepts are linear, indicating that $\beta = 0$ and giving kinetic constants of $K_i = 5.0$ mM and $\alpha = 3$. That is, there is no catalysis from the C·I·S intermediate.

These data suggested evaluation of other common Lewis basic ligands as inhibitors. Ethers and ketones were used to inhibit the rhodium octanoate-catalyzed reaction of the more readily accessible **1**, with the results summarized in Table 6. In all cases, $\beta = 0$.

Table 6. Analysis of Inhibition of the Reaction of **1** Catalyzed by Rhodium Octanoate Using Scheme 7

Lewis base	K_{i1} (mM)	K_{i2} (mM)	α
tetrahydrofuran	5.29	74.8	12.9
1,4-dioxane	27.9	114	4.1
acetone	5.00	81.8	0.52
cyclobutanone[a]	134		∞
cyclopentanone[a]	14.85		∞
cyclohexanone	55.4	70.3	1.27
methyl cyclopropyl ketone	196	1.21	0.0062
1-indanone	76.2	26.9	0.35
1,1,1-trifluoroacetone	258	328	1.27

[a] Competitive inhibitor.

Table 7. Saturation Kinetic Parameters for Rhodium Acetate-Catalyzed Reactions of Varied Diazocarbonyls[a]

reactant/catalyst	K_m(app) (mM)	k_{cat} (s^{-1})	k_{cat}/K_m ($M^{-1}s^{-1}$)
1/Rh_2Ac_4	1.14×10^3	3.3×10	2.9×10^1
9/Rh_2Ac_4	2.92×10^2	1.1×10^{-1}	3.6×10^{-1}
11/Rh_2Ac_4	3.01×10	8.9×10^{-2}	3.0

[a] Dioxane solvent, 60.0 °C.

In simple competitive inhibition, the K_i for a particular inhibitor/catalyst combination should be the same no matter which reaction is being catalyzed. With mixed inhibition, matters are not so simple, since another species to which the inhibitor may bind, C·S, is different when S is different. An inhibition study was therefore conducted with the same catalyst/inhibitor combination, but with three different substrates (**1**, **9**, and **11**). In this case the catalyst was $Rh_2(OAc)_4$ and 1,4-dioxane was used as the solvent (inhibitor). To make the rates measurable, the reactions were carried out at elevated temperature (60.0 °C). This experiment also addresses the issue raised earlier concerning catalyst desolvation being rate determining. The concentration of neat dioxane is 11.7 M, so far above the K_{i2} measured above that the catalyst must be doubly solvated in the resting state, and at least one dioxane must dissociate for any catalysis to occur. The data are summarized in Table 7. When the kinetic constants were measured in a noncoordinating solvent, such as CH_2Cl_2 (Table 3), the observed sequence of K_ms is K_m(**9**) > K_m(**11**) > K_m(**1**). In the coordinating solvent 1,4-dioxane, the measured parameter is K_m(app) because the reaction is inhibited (and must be run at higher temperature). The observed sequence of K_m(app) is K_m(**1**) > K_m(**9**) > K_m(**11**), which is neither a simple repeat nor the reverse of the sequence in CH_2Cl_2.

Discussion

This work establishes that dirhodium carboxylate-catalyzed reactions exhibit saturation kinetics and can be studied in detail using this formalism. The agreement of the kinetic parameters between the Büchner and cyclopropanation reactions eliminates rapid bimolecular formation of the norcaradiene intermediate followed by slow ring opening to the observed product as an alternative explanation for saturation, since no following reaction is involved in the cyclopropanation reaction. The data of Table 7 provide further evidence that the saturation kinetics cannot be attributed to dissociation of solvent from the catalyst, since if this were so, all three reactants should exhibit the same K_m(app). The electron-deficient catalyst rhodium trichloroacetate

Chart 1

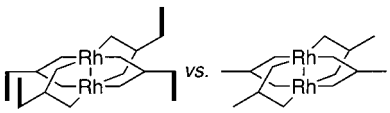

is better at binding diazocompound **1** than rhodium pivalate (K_m = 1.0 mM vs 15 mM), due to increased Lewis acidity, but is slightly slower in the catalytic step of nitrogen loss (k_{cat} = 625 s^{-1} vs 1100 s^{-1} for rhodium pivalate). This observation provides further support for our previous linear free energy relationship study that shows significant back-bonding from the metal to the carbene.[37] This back-bonding would tend to stabilize the carbene and facilitate its formation. Recent theoretical study has supported the ability of the dirhodium core to participate in back-bonding with good π-acid ligands,[38] though earlier studies had not found back-bonding.[39] The more electron deficient catalyst has a nearly 10-fold increase in overall rate due to its 15-fold stronger substrate binding, as is apparent in the second-order rate constants given in Table 2. The substrate inhibition of these reactions was surprising and sounds a cautionary note concerning preparative rhodium-catalyzed reactions conducted at high substrate concentrations or with electron-deficient catalysts. The divergence of the effects of catalyst on k_{cat}/K_m and on $K_{i(S)}$ for **1** support the idea that they address two different processes, one being binding of the diazo carbon to the catalyst and the other binding of the aromatic ring.

The diazo compounds studied in Table 3 demonstrate an interesting trend. As the pK_a of the carbon acid from which the diazo compound was derived decreases (ketone pK_a > β-ketoester pK_a > β-diketone pK_a), k_{cat}/K_m decreases. The rate of the reaction of **13** was too fast to be measurable, but is clearly faster than **1**. Since an ester α-C−H bond is less acidic than a ketone α-C−H bond, this observation reinforces the trend. Our interpretation of this overall phenomenon is that the diazo carbon is more basic when adjacent to poorer anion-stabilizing groups and therefore a better donor to rhodium in the initial association step (neglecting steric effects).

A great deal can be learned about the electronic influence of ligands on selectivity in rhodium-catalyzed reactions through extensive catalyst variation and linear free energy relationship analysis.[37,40] An important result of such studies was demonstration of the significance of rhodium-to-carbenoid back-bonding. A much smaller study of the effect of ligands on kinetic parameters is reflected in Table 5. Given the 4 orders of magnitude in variation of the ligand's conjugate acid pK_a, the almost identical selectivity constants for these reactions are startling. These data suggest that changing the rhodium ligands to affect reaction selectivity should not strongly affect the ability of the catalyst to catalyze reactions of diazo compounds. The large literature on synthetic reactions exhibiting just this behavior is reassuring regarding the results of the kinetic study, which reiterate these observations.

The slower rate of the reaction of **15** catalyzed by the chiral Rh_2(DOSP)$_4$ catalyst as compared to the two achiral catalysts is consistent with the reactivity/selectivity principle. That the chiral catalyst is approximately half the rate of the achiral catalysts may be a statistical effect related to the D_2 catalyst symmetry, which sterically permits only four approach vectors to the rhodium, whereas the achiral catalysts permit eight (Chart 1). Our other study shows that there is little effect of the catalyst carboxylate ligand pK_a on the kinetics.

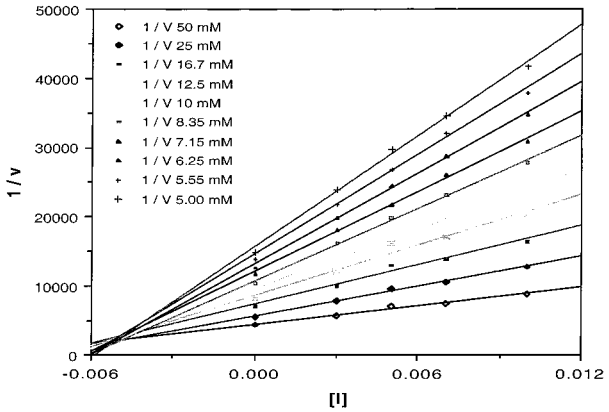

Figure 5. Plot of $1/v$ vs [I] at constant [S] for rhodium pivalate-catalyzed reaction of **5** in the presence of acetonitrile.

The mixed inhibition demonstrated in these rhodium-catalyzed reactions is consistent with their kinetic complexity due to the dual binding sites. Inhibition by even weak Lewis acids serves as a caution to experimenters conducting rhodium-catalyzed reactions preparatively—functional groups often present in substrates (aromatic rings!) or minor amounts of common solvents can clearly affect reaction rates. The kinetically determined inhibition constant for acetonitrile binding to rhodium pivalate (5 mM) compares to a spectroscopically determined value of 0.9 mM for the first acetonitrile binding to rhodium butyrate[33] and is significantly below the second binding constant (90 mM). The magnitude of α suggests that the top line of Scheme 7 carries most of the flux at reasonable substrate concentrations since αK_{i1} = 15 mM and αK_m = 36 mM. The concentration of C·I·S is not significant at these substrate and inhibitor concentrations (by assuming that $K_{i2} \gg K_{i1}$ and that β = 0, [C·I·S] can be calculated to be 6% of the total catalyst). Because of this, β need not be truly zero, since the second line is not highly populated at these inhibitor concentrations, and it would have a small effect on the rate. Further evidence that the second binding of the inhibitor is not kinetically significant at these inhibitor concentrations comes from plotting $1/v$ vs [I] at a constant [S], as shown in Figure 5. A deviation from linearity would indicate that the second binding step was occurring, and these plots are linear at the concentrations studied.

Because these dirhodium complexes have two open coordination sites, they might be thought to catalyze reactions at both sites simultaneously. That the second catalytic site becomes less efficient when even a weak ligand (inhibitor) is bound at the other site suggests that the presence of a carbenoid at one site would significantly inhibit binding and thereby retard catalysis at the other site. It is not possible to use kinetics to measure the strength of the binding once the carbenoid is formed, but it is expected to be quite strong. Strong binding of the carbenoid would disfavor the binding of a second diazo compound through the trans effect. If only one site functions at a time as described, these complexes could be considered to exhibit "half-of-the-sites" activity like many enzymes, an extreme example of

(37) Pirrung, M. C.; Morehead, A. T. *J. Am. Chem. Soc.* **1994**, *116*, 8991−8.
(38) Sargent, A. L.; Rollog, M. E.; Eagle, C. T. *Theor. Chem. Acc.* **1997**, *97*, 283−8.
(39) Bursten, B. E.; Cotton, F. A. *Inorg. Chem.* **1981**, *20*, 3042.
(40) Wang, J.; Chen, B.; Bao, J. *J. Org. Chem.* **1998**, *63*, 1853−62.

Chart 2

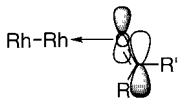

Table 8. DFT-Calculated Frontier Molecular Orbital Energies and α Values for Carbonyl Inhibitors of Dirhodium Carboxylate-Catalyzed Reactions

ketone	E_{LUMO} (eV)	E_{HOMO} (eV)	α
methyl cyclopropyl ketone	−1.7	−5.82	0.0062
acetone	−1.9	−5.82	0.52
1-indanone	−2.8	−5.77	0.35
cyclohexanone	−1.9	−5.55	1.27
1,1,1-trifluoroacetone	−3.2	−6.97	1.27

negative cooperativity in the binding step.[41] Our data suggest that the kinetically most efficient pathway involves only one carbenoid ligand per dirhodium catalyst.

A more subtle mechanistic point is that dissociation of a carboxylate to open another coordination site is not likely, since these data indicate only one binding site for inhibition, rather than multiple sites, as would be expected if another coordination site is opened. The dissociative mechanism of Alonso and García is also strongly disfavored by these findings, since the K_i and k_{cat} for a monomer would be expected to react differently to the inhibitor than the dimer, leading to a nonlinearity of the replots of v vs [I] (analogous to a catalytically active and significant concentration of a C·I·S complex).

A notable feature of the data in Table 6 is that acetone has an α value less than 1. This indicates that acetone prefers to bind to the substrate-bound form of the catalyst (or the carbenoid) rather than the free catalyst. However, it should be emphasized that β is still 0, so that the C·I·S complex formed must lose acetone to catalyze the reaction. Efforts to further understand this phenomenon through variation of the carbonyl basicity and π-bond strength were frustrated by the fact that cyclobutanone and cyclopentanone do not show mixed inhibition ($\alpha = \infty$). Rather, they are pure competitive inhibitors. Two other ketones, indanone and methyl cyclopropyl ketone, were also found to exhibit an α value less than 1. This phenomenon might be explained as shown in Chart 2. The carbonyl is bound to the rhodium through an unshared pair, but unlike most other inhibitors is capable of back-bonding. This may reduce its trans effect, which may permit binding of a ligand at the other axial coordination site of the dirhodium core or, conversely, that its trans effect is reduced by back-bonding may permit its binding when another strong trans effect ligand is already bound. This explanation suggests a correlation of the back-bonding ability of the carbonyl to the α value. To examine this idea, the LUMO energies of the five carbonyl compounds exhibiting mixed inhibition were obtained by DFT methods, as summarized in Table 8. These data are confusing at best. To be sure, calculated LUMO energies are approximate at best, and the correlation between LUMO energies and α is clearly not direct. Steric factors and HOMO energies (correlating to the strength of the carbonyl−rhodium association) may also be important to this model. Back-bonding may be the basis for the unusual inhibition behavior of some ketones, but inhibition by others may have a different basis. Carbonyls, as electron-deficient π-bonds, may bind *only* as acceptors for the significantly enhanced electron density at the free rhodium when a ligand is bound to the distal rhodium. This explanation predicts that other electron-deficient π-bonds should exhibit similar behavior. Finally, it may be possible that certain ketones inhibit the reaction by binding directly to the carbenoid carbon. The intramolecular coordination/binding of an ester/lactone carbonyl to a carbenoid carbon has been used to explain the high enantioselectivity in rhodium-mediated reactions of lactate/pantolactone diazoesters.[42] If this were the case, the donor ability of the ketone as reflected in its HOMO energy should be key. The DFT-calculated HOMO energies of this group of ketones also provided in Table 8 do not support this model, however. Indanone also has another potential binding site for rhodium, the aromatic ring. Based on our earlier results showing that unhindered and electron-rich aromatic rings have greater affinity for dirhodium carboxylates, it seems unlikely that the electron-deficient aromatic ring of indanone would be a good ligand for rhodium octanoate.

The proposal of Alonso and García,[25] who postulated that nitrogen is not lost in the rate-determining step because of the large negative entropy of activation found in their kinetic study is in direct opposition to our proposal for the mechanism of dirhodium carboxylate-catalyzed reactions. However, it should be noted that a bimolecular C−H insertion reaction could quite possibly have a different rate-determining step. The C−H insertion reaction would likely have a high entropy of activation due to the constrained approach of the C−H bond to the carbenoid, which would cost both translational and vibrational entropy in the transition state. However, we did observe valid saturation kinetics in the bimolecular C−H insertion reaction of **15**. The demonstration of the first-order dependence on rhodium acetate of the cyclopropanation of styrene by ethyl diazoacetate by Hubert and Noels is consistent with our proposal, since the study was performed at saturating concentrations of ethyl diazoacetate.[24]

Applying the Yates model and our kinetics to these reactions, the relative energies of certain intermediates and transition states in the rhodium pivalate-catalyzed reaction of **1** can be estimated (Figure 6). If K_m is assumed to be equal to K_s, the relation $\Delta G = -RT \ln K_m$ may be used to show that the catalyst/diazocarbonyl complex (C·S) is 2.5 kcal/mol lower in energy than the starting materials (using $K_m = 15$ mM). The use of $K_m \approx K_s$ assumes that $k_{cat} \ll k_{-1}$, a presumption supported by the known off rates of water and acetonitrile,[33] which must be greater than 10^5−10^6 M^{-1} s^{-1}, the rate at which phosphine and nitrogen adducts are formed in water and acetonitrile solution by a dissociative process. These rates are several orders of magnitude higher than k_{cat} (≈1100). Since K_m will always be larger than K_s (Supporting Information), 2.5 kcal/mol is the lower limit on the binding energy. Application of the Eyring equation to k_{cat} allows calculation of the $\Delta G^{\ddagger}$ for loss for nitrogen from the bound intermediate to be 13.3 kcal/mol (for $k_{cat} = 1100$ s^{-1}). The loss of nitrogen in this step effectively makes it irreversible. No inference can be made about the relative energy of the metal−carbene complex or the transition state for formation of the initial catalyst/diazocarbonyl complex from these data.

(41) Seydoux, F.; Malhotra, O. P.; Bernhard, S. A. *Crit. Rev. Biochem.* **1974**, *2*, 227.

(42) Davies, H. M. L.; Huby, N. J. S.; Cantrell, W. R., Jr.; Olive, J. L. *J. Am. Chem. Soc.* **1993**, *115*, 9468−79.

(43) Guthikonda, G. N.; Cama, L. D.; Christensen, B. G. *J. Am. Chem. Soc.* **1974**, *96*, 7584−5.

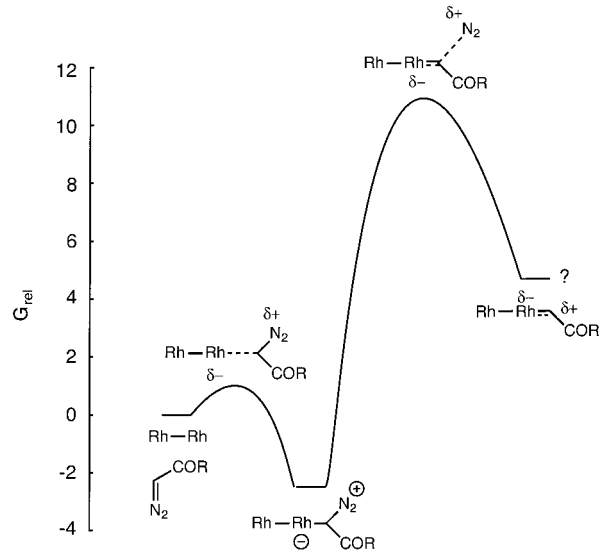

Figure 6. Free energy profile for the rhodium pivalate-catalyzed reaction of **1**.

The second-order rate constants measured for the rhodium-catalyzed reactions reported in this paper are as high as 10^5 M^{-1} s^{-1}. While far superior to the other catalytic chemical reactions whose saturation kinetic parameters have been determined, and certainly fast enough to qualify rhodium carboxylates as chemzymes, clearly they also require significant enhancement to reach the "catalytic perfection" of diffusion-controlled reactions. Furthermore, the introduction of chirality into this catalyst framework has the effect of slowing the catalytic process (by about half). A reasonable suggestion is that this is due to blockage of enantiotopic catalytic sites in an achiral catalyst framework. While the concept of asymmetric ligand-accelerated catalysis has certainly been powerful in developing catalytic asymmetric reactions, asymmetric catalysis may also involve ligand-*decelerated* catalysis by steric blockage of one of the two enantiotopic pathways. Detailed kinetic analyses of chiral and comparable achiral catalysts, such as we have performed here for $Rh_2(DOSP)_4$, will be required to assess this factor in other catalytic systems.

Experimental Section

Known compounds are as follows: 1-diazo-4-phenyl-2-butanone (**1**), 3,8a-dihydro-1(2*H*)-azulenone (**2**), 1-diazo-4-(4-methoxyphenyl)-2-butanone (**3**), and 3,8a-dihydro-6-methoxy-1(2*H*)-azulenone (**4**).[36] Also known are 1-diazo-5-hexen-2-one (**7**)[43] and bicyclo[3.1.0]hexan-2-one (**8**).[44]

1-Diazo-4-methyl-4-phenylpentan-2-one (5). Oxalyl chloride (3.05 g, 2.10 mL, 24.0 mmol) was added to 3.56 g (20.0 mmol) of 3-methyl-3-phenylbutanoic acid in 50 mL of Et_2O under Ar, followed by one drop of dimethylformamide (DMF; gas evolution). After stirring for 1 h, the solvent was removed under vacuum to leave a clear oil. The oil was dissolved in 50 mL of Et_2O and transferred to a 250 mL Erlenmeyer flask and immediately treated with approximately 50 mmol of CH_2N_2 in Et_2O. After 1 h, the solvent was removed under vacuum and the residual yellow oil was chromatographed on silica gel using 2:1 hexane:ethyl acetate. The solvent was removed under vacuum to give 3.60 g (17.8 mmol, 89%) of a clear yellow oil. ^{1}H NMR ($CDCl_3$): δ 1.45 (s, 6H), 2.60 (s, 2H), 4.66 (s, 1H), 7.24 (dd, J = 8.7, 7.2 Hz, 1H), 7.35 (m, 4H). ^{13}C NMR ($CDCl_3$): δ 28.7, 37.8, 54.9, 55.4, 125.2, 125.4, 126.0, 128.2, 128.3, 147.8, 193.3. IR (thin film): 2936, 2103, 1635 cm^{-1}. HRMS for $C_{12}H_{15}N_2O$ (FAB^+, MH^+). Calcd: 203.1186. Found: 203.1184.

3,8a-Dihydro-2,2-dimethyl-1(2*H*)-azulenone (6). 1-Diazo 4-methyl 4-phenylpentan-2-one (100.2 mg, 0.495 mmol) was dissolved in 50 mL of CH_2Cl_2 and treated with 1.5 mg (0.0025 mmol) of rhodium pivalate. After stirring for 30 min, the solvent was removed under vacuum and the residue was filtered through a short plug of silica gel to give 82.7 mg (0.474 mmol, 96%) of a clear oil. ^{1}H NMR ($CDCl_3$): δ 1.14 (s, 3H), 1.40 (s, 3H), 2.35 (d, J = 16.8 Hz, 1H), 2.59 (dd, J = 16.9 Hz, 0.7 Hz, 1H), 2.89 (m, 1H), 5.19 (dd, J = 9.4, 4.1 Hz, 1H), 6.14 (ddd, J = 9.3, 5.7, 1.8 Hz, 1H), 6.20 (dd, J = 5.7, 1.5 Hz, 1H), 6.43 (dd, J = 11.1, 5.7 Hz, 1H), 6.53 (dd, J = 11.1, 5.7 Hz, 1H). ^{13}C NMR ($CDCl_3$): δ 27.3, 32.9, 40.1, 51.4, 54.1, 117.0, 119.8, 126.7, 129.7, 130.3, 148.5, 216.1. IR (thin film): 2960, 2867, 1747 cm^{-1}. HRMS for $C_{12}H_{14}O$ (EI, 70 eV). Calcd: 174.1045. Found: 174.1049.

2-Diazo-3-oxododecanoic Acid Methyl Ester (9). NaH (1.22 g, 60% in mineral oil, 30.6 mmol) was placed in a 100 mL round-bottom flask and suspended in 50 mL of dry tetrahydrfuran (THF) under nitrogen. Methyl acetoacetate (3.00 mL, 27.8 mmol) was added slowly to the suspension at 0 °C. The mixture turned from cloudy suspension to a clear solution upon completion of addition. Then *n*-BuLi (19.1 mL, 1.6 M in hexane, 30.6 mmol) was added at 0 °C over 15 min, and the solution turned orange. The solution was stirred for an additional 10 min before 1-bromooctane was added, and the mixture was stirred overnight. The reaction was quenched with 4 mL of concentrated HCl in 10 mL of water and 25 mL of ether. The aqueous layer was extracted with ether (25 mL × 2). The combined organic phase was washed with brine until neutral, and the solvent was removed under vacuum. The crude product was purified by flash chromatography (R_f = 0.25, 1:9 ethyl acetate:hexane) to obtain the alkylated product as a clear oil (4.12 g, 82%). ^{1}H NMR ($CDCl_3$): δ 0.85 (t, J = 6.30 Hz, 3H), 1.24 (br s, 12H), 1.56 (m, 2H), 2.50 (t, J = 7.2 Hz, 2H), 3.42 (s, 2H), 3.71 (s, 3H).

The alkylated product, 3-oxododecanoic acid methyl ester, was subjected to a diazo transfer procedure. The ester (4.12 g, 18.0 mmol) and mesyl azide (1.72 mL, 19.8 mmol) were dissolved in 20 mL of dry acetonitrile under nitrogen, to which solution Et_3N (2.76 mL, 19.8 mmol) was added at room temperature. The solution was stirred for 6 h. The solvent was removed under vacuum. The residue was redissolved in 20 mL of ether and washed sequentially with NaOH (10% aq, 20 mL × 2), brine twice, dried over Na_2SO_4, filtered, and evaporated. The product was purified by chromatography (R_f = 0.52, 1:4 ethyl acetate:hexane) and obtained as a yellow oil (3.70 g, 81%). ^{1}H NMR ($CDCl_3$): δ 0.85 (t, J = 6.9 Hz, 3H), 1.24 (m, 12H), 1.60 (m, 2H), 2.81 (t, J = 7.2 Hz, 2H), 3.81 (s, 3H). ^{13}C NMR ($CDCl_3$): δ 14.19, 22.74, 24.46, 29.33, 29.46, 29.51, 31.93, 40.27, 52.14, 76.80, 77.21, 161.64, 192.75. IR (thin film): 2135, 1718, 1653 cm^{-1}. HRMS for $C_{13}H_{22}N_2O_3$ (EI, 30 eV, M^+). Calcd: 254.1630. Found: 254.1640.

2-Hexyl-5-oxocyclopentanecarboxylic Acid Methyl Ester (10). Compound **9** (222.3 mg, 0.87 mmol) was dissolved in 25 mL of dry CH_2Cl_2. To this solution at room temperature rhodium acetate (4.5 mg, 0.01 mmol) was added. The solution was stirred at room temperature for 2 h, and the solvent was removed under vacuum. The crude product was flash chromatographed (R_f = 0.20 1:9 ethyl acetate:hexane) to obtain **10** as a clear oil (162.2 mg, 82%). ^{1}H NMR ($CDCl_3$): δ 0.86 (t, J = 6.9 Hz, 3H), 1.25−1.52 (m, 12H), 2.15−2.60 (m, 3H), 2.81 (d, J = 11.4 Hz, 1H), 3.74 (s, 3H). ^{13}C NMR ($CDCl_3$): δ 13.97, 22.50, 27.05, 27.28, 29.21, 31.63, 34.91, 38.40, 41.37, 52.28, 61.83, 169.97, 211.91. IR (thin film): 1750, 1725 cm^{-1}. HRMS for $C_{13}H_{22}O_3$ (EI, 30 eV, M^+). Calcd: 226.1569. Found: 226.1561.

3-Diazotridecane-2,4-dione (11). ^{1}H NMR ($CDCl_3$): δ 0.88 (t, J = 6.6 Hz, 3H), 1.27 (m, 12H), 1.65 (quintet, J = 7.5 Hz, 2H), 2.45 (s, 3H), 2.70 (t, J = 7.5 Hz, 2H). ^{13}C NMR ($CDCl_3$): δ 14.15, 22.70, 24.16, 28.68, 29.18, 29.20, 29.40, 29.44, 31.88, 40.61, 83.83, 188.38,

(44) Newman-Evans, R. H.; Simon, R. J.; Carpenter, B. K. *J. Org. Chem.* **1990**, *55*, 695−711.

190.79. IR (thin film): 2217, 1650 cm^{-1}. HRMS for $C_{13}H_{22}N_2O_2$ (EI, 30 eV, M^+). Calcd: 238.1681. Found: 238.1675.

2-Acetyl-3-hexylcyclopentanone (12). ^1H NMR ($CDCl_3$; 2:1 diketo and enolic forms): δ 0.86 (t, $J = 6.3$ Hz, 1H), 0.87 (t, $J = 6.9$ Hz, 2H), 1.25−1.50 (m, 11H), 1.67−1.75 (m, 0.33H), 1.89−2.04 (m, 1.66H), 2.11−2.35 (M, 3.66 H), 2.42−2.56 (m, 0.33H), 2.61−2.70 (m, 0.33H), 2.75−2.84 (m, 0.33H), 3.01 (d, $J = 10.5$ Hz, 0.33H), 5.28 (s, 0.33H). ^{13}C NMR ($CDCl_3$): δ 14.14, 20.44, 22.65, 23.16, 25,91, 26.85, 27,17, 27.46, 27.83, 29.39, 29.48, 29.98, 30.63, 31.09, 31.77, 31.92, 32.84, 35.17, 35.52, 38.39, 38.96, 39.03, 48.75, 69.44, 114.85, 175.59, 202.84, 205.86, 212.46. IR (thin film): 3100, 1739, 1708 cm^{-1}. HRMS for $C_{13}H_{22}O_2$ (EI, 30 eV, M^+). Calcd: 210.1620. Found: 210.1628.

General Procedures for Saturation Kinetics. All UV measurements were conducted on a Shimadzu UV160U instrument. For reactions with stable reactants and products, pure compounds were used for the measurement of their UV spectra from 200 to 400 nm. The single wavelength for following the reaction was chosen by two criteria, where their absorbance has the biggest difference and where both UV spectra are as flat as possible, so that the effect of instrumental fluctuations would be minimal. The extinction coefficients of both reactant and product at this wavelength were measured and used in the calculation of reaction rate. For reactions conducted at high substrate concentration, for example to determine substrate K_is, it was necessary to use longer wavelengths at which the total absorbance was lower.

A stock solution of each diazo compound and catalyst was prepared in a volumetric flask using CH_2Cl_2. Addition of the appropriate volume of the stock solution of diazo compound and dilution with CH_2Cl_2 to a volume of 3.000 mL by using Hamilton syringes in a quartz cell (10 mm path length) was performed for each rate determination. The capped cells were equilibrated to 25.0 °C (28.0 °C for rates in Table 2 and otherwise noted) before the catalyst was introduced. Addition of an aliquot of catalyst solution (concentration of catalyst in the reaction after addition was 2.00×10^{-7} M) and mixing using a disposable pipet or the tip of the Hamilton syringe was followed by determination of the rate by monitoring the change in absorbance at the appropriate wavelength (see Table 9 for measured UV absorbances) at 1 s intervals. Linear least squares line fit (using the Shimadzu UV160 software line fitting function) to at least 20 points were used to determine initial velocities. For the inhibition analysis, the appropriate volume of a stock solution of inhibitor in CH_2Cl_2 was added to the diazo compound solution before diluting to 3.000 mL in an analogous manner.

The slope of the straight line fitting the raw data was used to calculate the rates. The velocities were scaled to the appropriate units (M s^{-1}) by applying eq 1, easily derived from Beer's Law with the assumption that the reaction proceeds in quantitative yield.

Table 9. Absorption Properties of Reactants and Products in Kinetic Studies

compds	λ (nm)	ϵ_p ($M^{-1}cm^{-1}$)	ϵ_r ($M^{-1}cm^{-1}$)
1 and **2**	340	186.8	37.2
3 and **4**	360	175.0	91.6
5 and **6**	340	106.8	23.0
7 and **8**	370	11.0	30.0
9 and **10**	340	9.40	31.8
11 and **12**	360	2.39	36.8
15 and **16**	330	39.7	260

$$d[S]/dt = (dA/dt)/\{(\epsilon_p - \epsilon_r)l\} \quad (1)$$

where ϵ_p and ϵ_r are the extinction coefficients of the product and reactant, dA/dt is the rate of change of the absorbance, and l is the path length in centimeters.

For inhibition studies, normal rectangular hyperbolae were converted to Lineweaver−Burk plots. All straight lines for different inhibitor concentrations were plotted on the same plot. The type of inhibition can be determined according to the position of their intersection point. Most of our inhibition studies showed mixed inhibition (intersection to the left of the *y*-axis, not on the *x*-axis), which can be described by

$$v = \{V/(1 + [I]/K_{i2})\}/\{1 + [K_m(1 + [I]/K_{i1})]/[[S](1 + [I]/K_{i2})]\} \quad (2)$$

In this case, secondary plots are required to determine the inhibition constants. The intercept of the secondary plot of the slopes vs [I] is K_{i1}. The intercept of the secondary plot of the intercept on the vertical axis in the v vs [S] plots is K_{i2}.

Acknowledgment. This work was supported by the donors of the Petroleum Research Fund, administered by the American Chemical Society (ACS). A.T.M. was a C. R. Hauser Fellow and an ACS Division of Organic Chemistry Upjohn Graduate Fellow.

Note Added after ASAP: There was an incorrect α value in the version posted ASAP January 19, 2002; the corrected version was posted February 6, 2002.

Supporting Information Available: Saturation kinetic analysis, additional kinetic plots, NMR spectra for **5**, **6**, and **9**−**12** (PDF). This material is available free of charge via the Internet at http://pubs.acs.org.

JA011599L